THE JOURNAL OF PHYSICAL CHEMISTRY B

Article

pubs.acs.org/JPCB

Conduction in a Biological Sodium Selective Channel

Letícia Stock,[†,§] Lucie Delemotte,[‡,§] Vincenzo Carnevale,[*,‡] Werner Treptow,[*,†,‡] and Michael L. Klein[‡]

[†]Laboratório de Biofísica Teórica e Computacional, Departamento de Biologia Celular, Universidade de Brasília DF, Brasil

[‡]Institute of Computational and Molecular Science, Temple University, Philadelphia, Pennsylvania 19122, United States

Supporting Information

ABSTRACT: The crystal structure of NavAb, a bacterial voltage gated Na^+ channel, exhibits a selectivity filter (SF) wider than that of K^+ channels. This new structure provides the opportunity to explore the mechanism of conduction and help rationalize its selectivity for sodium. Recent molecular dynamics (MD) simulations of single- and two-ion permeation processes have revealed that a partially hydrated Na^+ permeates the channel by exploring three SF binding sites while being loosely coupled to other ions and/or water molecules; a finding that differs significantly from the behavior of K^+ selective channels. Herein, we present results derived from a combination of metadynamics and voltage-biased MD simulations that throws more light on the nature of the Na^+ conduction mechanism. Conduction under 0 mV bias explores several distinct pathways involving the binding of two ions to three possible SF sites. While these pathways are very similar to those observed in the presence of a negative potential (inward conduction), a completely different mechanism operates for outward conduction at positive potentials.

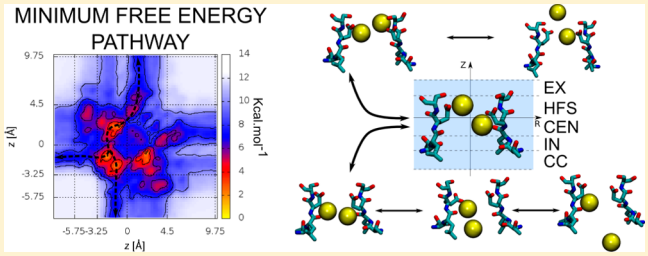

The functional viability of biological ion channels relies on their ability to conduct ions at a near-diffusion-limited rate as well as to discriminate between ionic species. These attributes are crucial for a variety of biological functions, including the propagation of nervous impulses, the control of osmotic pressure, and cellular contraction.[1] This remarkable behavior rests on the unique attributes of the structural motifs constituting their respective selectivity filters (SFs). Indeed, the presence of several polar/charged residues favors the partial desolvation of cations thereby ensuring a fast kinetics of permeation through the constricted region of the SF lumen.[2] Strikingly, similar ionic species can show permeation rates differing by, at least, 2 or 3 orders of magnitude. In general, passage of ions through the hydrophilic lumen of channels relies on a dynamic process of binding/dissociation to/from favorable SF binding sites. Subtle differences in the free-energy (FE) landscape describing this process for different ions results in significantly different permeation rates, providing a possible rationalization of selectivity.[3] To date, the mechanism of ionic conduction and selectivity operating in K^+ selective channels has been well characterized, as described extensively in recent reviews.[3−6]

The atomic structure of NavAb, a bacterial voltage-gated Na^+ channel, was reported recently.[7] This finding enables a deeper understanding of the function of the Nav family and the closely related Cav channels. Indeed, NavAb is one of the possible ancestors of the large family of vertebrate Nav and Cav channels,[8] providing us with a working model to characterize the molecular mechanisms underlying ionic conduction in a Na^+ selective channel. In contrast to the case of K^+ channels, the structure of the NavAb SF, formed by a tetrameric arrangement of the conserved sequence TLESWAS, features a pore 15 Å long that is large enough to accommodate a fully solvated cation (Figure 1A). The SF structure of NavAb exhibits a complex architecture formed by four layers of pore-lining oxygen ligands defining three putative sites for Na^+ binding, HFS, CEN, and IN, respectively, as originally envisioned by Payandeh et al.[7] The outermost site (HFS) is formed by the four negatively charged carboxyl groups involving the Glu177 side-chains and the hydroxyl groups of Ser178, whereas the other two sites, CEN and IN, are lined by the carbonyl groups of Leu176 and Thr175, respectively. The picture that emerged from K^+ channels of a rigid environment mimicking the first aqueous solvation shell[9] seems to be inappropriate for Na^+ channels, and most importantly, it is unable to rationalize selectivity.

Shortly after publication of the NavAb structure, several groups investigated independently the conduction mechanism of Na^+ across the SF of NavAb via MD simulations.[10−13] Studies relying on calculations of the potential of mean force (PMF) along the SF axis of symmetry (axial PMF) for a single Na^+ indicated that a single ion can bind the NavAb filter at sites HFS, CEN, and IN, providing support to the hypotheses of Payandeh et al.[11−13] As estimated from the axial PMFs, free-energy barriers in the range of 3−5 kcal/mol limit the diffusion of a single Na^+ through the SF of NavAb.[11−13] Although it may be possible for a single ion to overcome such an energy barrier, axial−axial PMF calculations for two Na^+ ions support the

Received: February 7, 2013
Revised: March 2, 2013
Published: March 3, 2013

   dx.doi.org/10.1021/jp401403b | J. Phys. Chem. B 2013, 117, 3782−3789

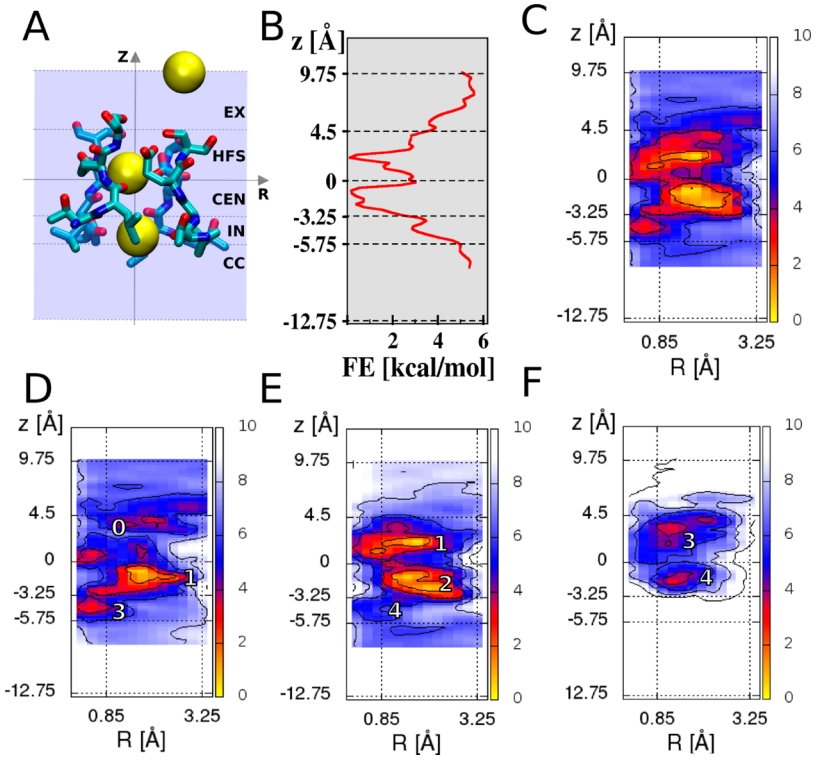

Figure 1. Binding of two Na^+ ions in the NavAb SF. (A) Available SF sites are: the external medium (EX); the central cavity (CC); plus the volumes enclosed by the ring of Glu177 carboxyls and Ser178 carbonyls (HFS); the carbonyls of Leu176 (CEN) and Thr175 (IN). (B) Axial and (C) radial-axial FE plots for Na^+ within the SF, highlighting three major binding sites, HFS (jointly off- and on-axis of symmetry), CEN (off-axis), and IN on-axis. Panels D−F are the conditional radial-axial FE surfaces describing the stability of a configuration with one ion at position (R, z) given that the other one is in site HFS (D), CEN (E), and IN (F), respectively. These surfaces reveal five local minima: HFS^2 (0), HFS-CEN (1), CEN^2 (2), HFS-IN (3), and CEN-IN (4). All FEs are in kcal/mol.

notion that conduction through NavAb involves the participation of an additional ion,[11,12] which is consistent with results by Carnevale et al. showing spontaneous SF occupation by two ions.[10] Thus, the emerging view to the conduction process is that of a SF preferentially occupied by two ions, which can switch between different configurations through a loosely coupled mechanism,[11,12] which is decoupled from water transport across the filter.[10] In spite of few inconsequential structural differences, this picture seems also to apply also to NavRh.[14]

Although the general features of conduction have been revealed, some questions remain unanswered. For instance, the binding affinity of Na^+ for each site when the SF is occupied by two ions remains unclear. Furthermore, the relative stability of all configurations accessible to a pair of SF-bound ions has not been characterized yet. Indeed, as discussed in details below, only a small fraction of two-ion configurations is present in the free-energy surfaces (FES) reported in the earlier works,[11,12] and therefore other potentially viable pathways of conduction were not sampled. Furthermore, the effect of the transmembrane potential on the conduction mechanism was explored only for the case of permeation of a single ion.[13] To shed light on these issues, we first characterize the relative stability of all configurations of a pair of Na^+ ions bound to the SF and then analyze the events underlying Na^+ translocation through the SF by employing nonequilibrium, voltage-driven MD simulations on the open-state structure of NavAb.[15] Importantly, the availability of a structural model of the open channel allows the study of conduction throughout the entire extension of the permeation pathway. In this fashion, subtle details of the process are revealed that were not evident in earlier studies based on the structure of the closed channel. The present study builds on insights from earlier computational investigations. Although there is overall consistency with the previous works, our picture of Na^+ conduction uncovers several previously unnoticed features.

RESULTS AND DISCUSSION

Two-Ion Conduction Mechanism on 4D Free-Energy Surfaces. Based on the X-ray structure of NavAb, we characterized the stability of all configurations of a pair of Na^+ bound to the SF and inferred the most probable conduction mechanism. For this purpose, metadynamics[16,17] was used to compute the FE as a function of the position of two ions. Two variables were chosen to locate the position of each ion: the distance along the SF axis of symmetry from the geometrical center of the Glu177 Cα residues (axial coordinate, z), and the distance from this axis (radial coordinate, R). The resulting 4-D FES was analyzed along several different subspaces by computing the corresponding marginal probability distribution functions.

The PMF as a function of the z coordinate of one ion (irrespective of its identity) shows consistently the anticipated picture of three binding sites HFS, CEN, and IN for $0 < z \leq 4.5$, $-3.25 < z \leq 0$, and $-5.75 < z \leq -3.25$, respectively (Figure 1). Sites HFS and CEN have similar energies (binding energies of ∼6 kcal/mol), whereas site IN (binding energy of ∼3 kcal/mol) corresponds to a less stable local minimum along z. When the FES is considered as a function of the z−R coordinates of one ion, one recovers the radial position of these sites. The

dx.doi.org/10.1021/jp401403b | J. Phys. Chem. B 2013, 117, 3782−3789

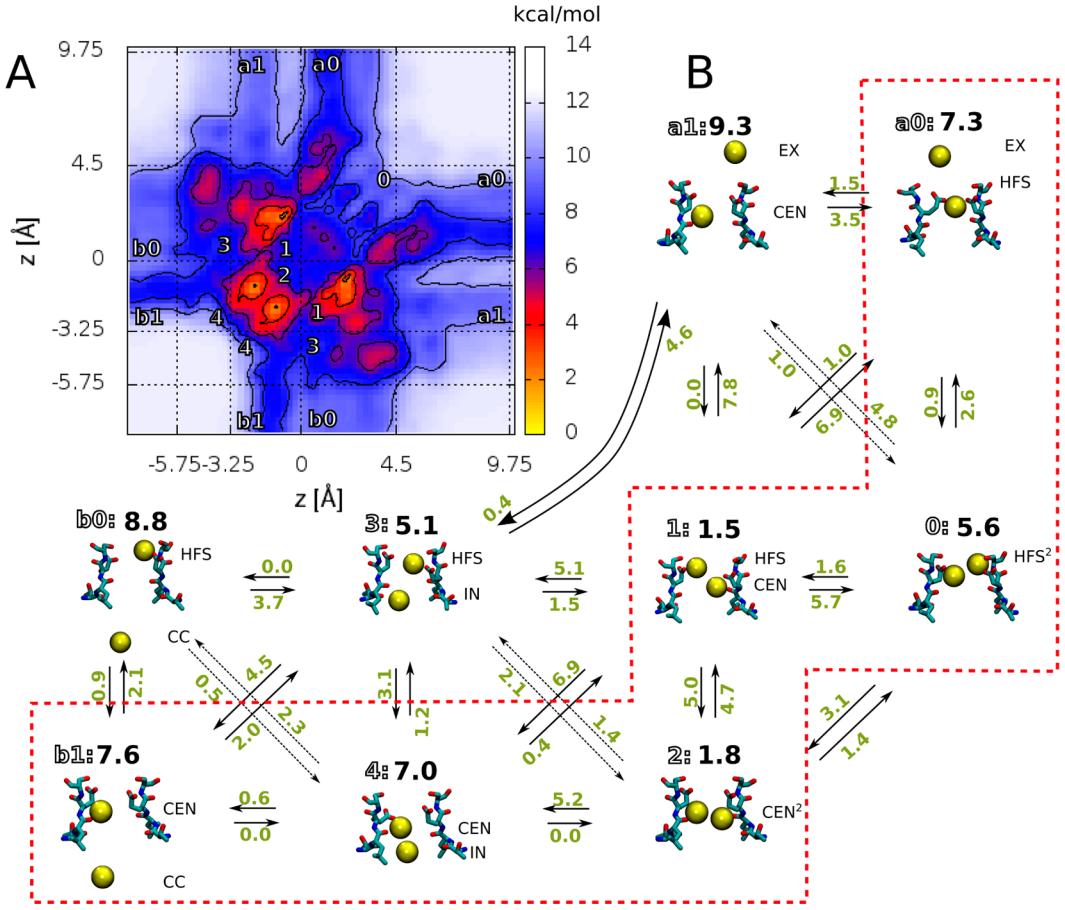

Figure 2. Two-ion conduction mechanism. (A) Symmetrized projection of 4-D free energy (kcal/mol) profile onto the two-ion axial−axial subspace, $G(z, z')$. (B) Five stable states (0 to 4) plus entry (a0, a1) and exit (b0, b1) configurations of two indistinguishable Na^+ ions along the SF symmetry axis. The FE and barriers for the forward and backward transitions are reported in black and green, respectively. The PMF is highlighted in red.

HFS site spans the entire range of radial distances, where a partially dehydrated ion binds to one or two Glu177-carboxyl groups. The CEN site is located off-axis, with the ion partially dehydrated and in close contact with one or two Leu176-carbonyl groups. The IN site lies close to the central axis, indicating that in this case the permeating ion retains its entire solvation shell. While validating the site positions previously reported by Carnevale et al.,[10] these FES provide further the binding energy of the ion in each site when two Na^+ occupy the filter. Note that the PMF results contrast with those obtained for a singly occupied SF, thereby highlighting the binding dependence with the number of SF-resident ions. For a singly occupied SF, all previous studies reported that, although a partially desolvated Na^+ sits off-axis at HFS by sticking to Glu177-carboxyl oxygens, a fully hydrated ion sits on-axis at sites CEN and IN, respectively. However, these studies provided a less consistent description of the relative stability of the different binding sites.[11−13]

To better characterize the FE of all of the configurations accessible to two ions, we computed the $z−R$ probability density functions for one ion conditioned on the position of the other one (Figure 1). Specifically, we considered three different probability density functions corresponding to configurations with one ion bound to HFS, CEN, or IN (hereafter, we use the superscript "2" to denote double occupancy of a site). The FES reveal five local minima: two deep ones (HFS-CEN and CEN^2) with free energy ∼−12.5 kcal/mol and three shallower ones (HFS^2, HFS-IN and CEN-IN with free-energy ∼−7 to −9 kcal/mol (in ref 12 HFS-CEN was also reported as the most stable state). Interestingly, the IN^2 state, i.e., a configuration with double occupancy of the IN site, does not exhibit a free-energy minimum, resulting from the on-axis location of the site. Note that these energies do not correspond to binding energies since the reference state is chosen here as the uppermost sampled configuration, in contrast to the case of the 1D-PMF in Figure 1B.

In the context of the 4-D FES, conduction of Na^+ through the SF is conceived as a connected path on the energy landscape joining two terminal states: one ion bound to the SF and the other one in the external medium (EX) and one ion bound to the SF and the other in the central cavity (CC), respectively. Given the directionality of Na^+ conduction through the SF, the diffusion process on this surface is best conveyed by a projection on the subspace spanned by the axial coordinates of the two indistinguishable ions (Figure 2). When mapped onto this space, states HFS^2, HFS-CEN, CEN^2, HFS-IN, and CEN-IN correspond to different ranges for the two axial coordinates, with the doubly occupied sites located approximately along the diagonal. We focus here on inward conduction but it is worth noting that outward conduction involves the reverse pathway. Entry to the SF from the EX occurs mostly through a pathway involving one ion in the HFS site and exit to the CC through a pathway involving one ion bound in the CEN site. Bridging between these entry and exit configurations, the presence of five stable states linked to each other by relatively low free-energy barriers (up to 6 kcal/mol)

dx.doi.org/10.1021/jp401403b | J. Phys. Chem. B 2013, 117, 3782−3789

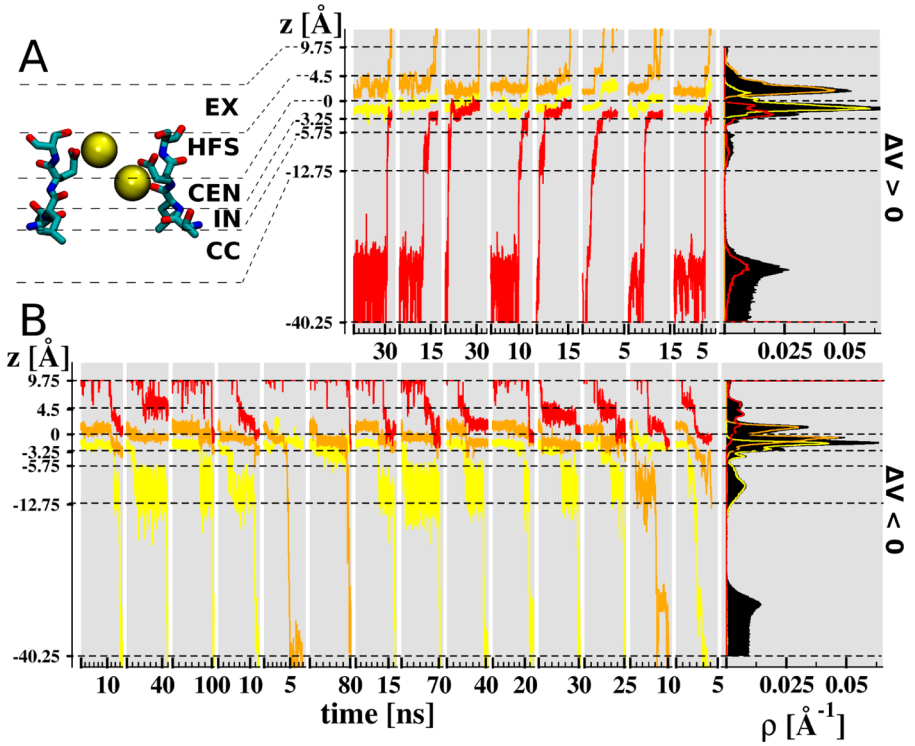

Figure 3. Membrane-polarized MD simulations of NavAb. (A) Trajectories of three Na^+: i (yellow), j (orange), and k (red) along the axial direction (z) under applied depolarization voltage differences ($\Delta V > 0$). Simulations start with ions j and i positioned, respectively at sites HFS and CEN of the SF (inset) and proceeds until complete delivery of either ion i or j to the external milieu. Ion k is the nearest external-bulk ion to the SF participating in the conduction event. The histogram of permeating ions calculated from the MD trajectories shows each of the i, j, and k densities (ρ) along the permeation pathway. Note that, the i, j, and k contribute mostly to the total Na^+-density (black) into the channel lumen. (B) Idem for conduction simulations under hyperpolarization conditions ($\Delta V < 0$). The bulk occupancy of ion "k" in the set of hyper- and depolarized simulations is shown as an occupancy peak at z = 9.75 Å (A) and z = −40.25 Å (B), respectively.

entails a plethora of productive pathways. However, the minimum-energy pathway (MEP), evidenced by a modified nudged elastic band method (See Methods for further details), involves sequential passage through four of the five states: HFS^2, HFS-CEN, CEN^2, and CEN-IN. Interestingly, the presence of minima along the diagonal of the axial−axial FES (states HFS^2 and CEN^2) ensures that the transport of Na^+ through the NavAb SF does not require forcing the preceding ion to leave: conduction may occur following the same MEP either through a knock-on or a drive-by mechanism in which the incoming ion proceeds unimpeded past the bound ion, stressing the 'loosely coupled' nature of the mechanism.

The present axial−axial FES can be compared directly with earlier works by Corry and Thomas[11] and Furini and Domene.[12] In the latter studies, conduction was reported to proceed preferentially through the pathway: EX-HFS ↔ HFS^2 ↔ HFS-CEN ↔ HFS-IN ↔ HFS-CC. Although we find that this pathway is one of the most probable (Figure 2), our results point to a distinct MEP involving double-ion occupancy of SF sites, i.e., EX-HFS ↔ HFS^2 ↔ HFS-CEN ↔ CEN^2 ↔ CEN-IN ↔ CEN-CC. This difference stems from the fact that in the previous studies only a portion of the entire range of possible axial displacements of the two sodium ions (z and z') was sampled. In Corry and Thomas[11] and Furini and Domene,[12] the two-ion axial−axial FES $G(z, z')$ was computed over $-10 \leq z \leq 17$ and $9 \leq z' \leq 25$, with the ion coordinates z and z' overlapping only within the SF region of site HFS and above. As such, the stability of some of the configurations of a pair of Na^+ ions bound to the SF was not determined, leading to a partial description of the conduction process.

Conduction Mechanism under TM-Voltage Potentials. In the following, we investigate the inward transport of ions through NavAb in a series of voltage-driven MD simulations of the full-length activated-open structure of the channel. Using a charge-imbalance protocol,[18] a (hyperpolarized) potential of ∼−600 mV was applied to the NavAb-membrane system in order to increase the rate of sampling of conduction events over these runs (cf. methods). Following this protocol, a set of 14 runs, starting with two ions in the SF at the HFS-CEN state, which according to our results is the global FE minimum at 0 mV, was carried out to sample inward conduction. The voltage-driven runs spanned a total of ∼0.5 μs.

From the simulations, the density profile for Na^+ along z features dominant peaks at HFS and CEN, and a small, yet resolved peak at IN (Figure 3). Further peaks are observed at EX, central cavity (CC) and activation gate (AG). Analysis of the number of oxygens in the first-coordination shell (3.1 Å cutoff) of Na^+ indicates hexa-coordination of the ion along the permeation pathway; only within the SF the ion is partially desolvated by SF-lining oxygen ligands. Overall, the axial-radial probability distribution $P(z, R)$ for Na^+ in the region of the SF agrees with the (0 mV) axial-radial FES in that it shows the on/off-, off-, and on-axis positions of sites HFS, CEN, and IN, respectively (Figure 1).

Integration of the density profile over the SF shows an average occupancy of ∼1.8 ions in the filter, implying that at negative voltages, conduction across the filter involves two SF-

dx.doi.org/10.1021/jp401403b | J. Phys. Chem. B 2013, 117, 3782−3789

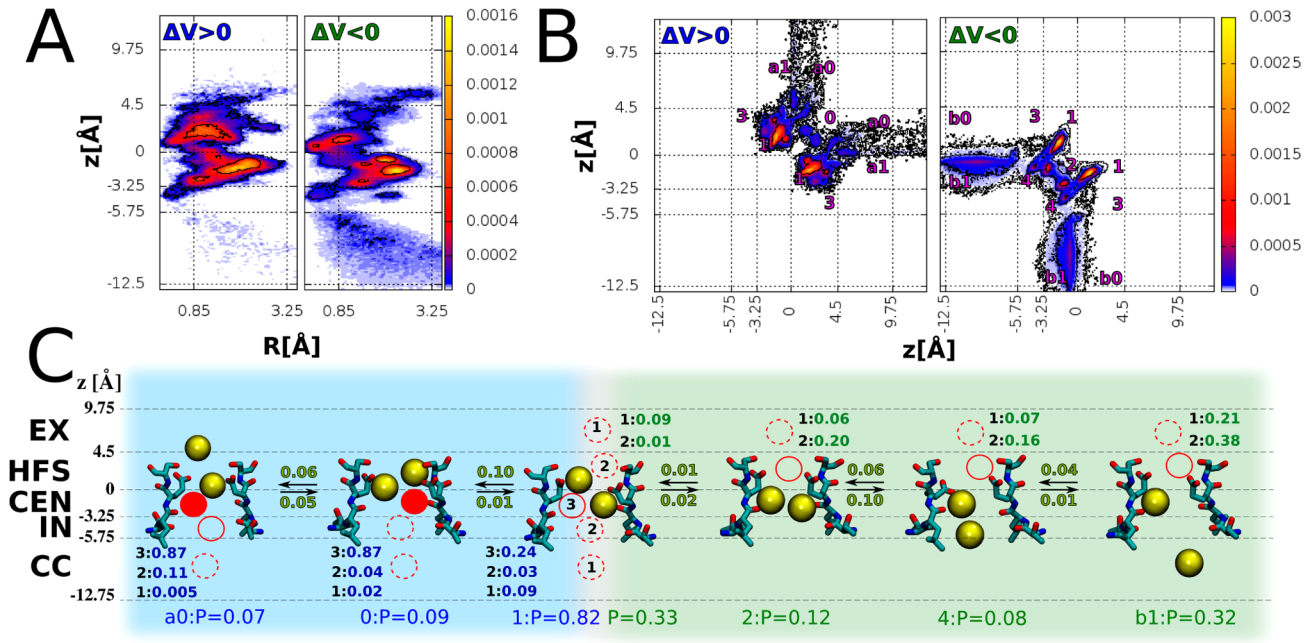

Figure 4. Sodium conduction under depolarized ($\Delta V > 0$) and hyperpolarized ($\Delta V < 0$) TM voltage differences. (A) Normalized axial-radial $P(z, r)$ and (B) axial−axial $P(z, z')$ probability distributions for ion occupancy at the NavAb filter. Both distributions were computed from data shown in Figure 2; $P(z, z')$ was symmetrized from the data by not distinguishing between ions i and j. (C) State (Ps) and forward/backward transition (Pwm) probabilities for the preferential conduction pathway under applied voltages, $\Delta V > 0$ (blue) and $\Delta V < 0$ (green). Starting from HFS-CEN (1), conduction proceeds inwardly via states CEN[2] (2), CEN-IN (4), and CEN-CC (b1) or outwardly via states HFS[2] (0) and HFS-EX (a0). For each of them, Ps was computed by integrating $P(z, z')$ over the domain $D = \{z, z'\}$ that maps the two-ion state in $G(z, z')$. Highlighted in red are the axial probabilities for ion k conditioned on the occupancy of state "s" of the SF-bound ions, $P_k(z|s)$; here, k is the ion closest to the SF participating in the conduction events. $P_k(z|s)$ is presented as the cumulative probability over the axial regions BULK, EX, HFS, and CC. Note that in the case of hyperpolarized runs, when the SF-bound ions are in the b1 configuration, ion k is likely to be found in site HFS suggesting a loose coupling with release of sodium into the CC, whereas in the case of depolarization conditions, $P_k(z|s)$, integrated over the CC or SF regions, highlights a strong coupling between the motion of k and the release of sodium into the bulk region.

bound ions. To characterize this two-ion process and its coupling to other ions, we focus our analysis on a three-ion ijk system. As indicated in Figure 3, ions i and j started the simulations in the filter whereas k is the ion closest to the SF that participates in the conduction event. Note that, within the filter and central cavity of the channel, the total-Na^+ density results mostly from contributions of these ions. The axial−axial probability distribution $P(z, z')$ for the SF-bound ions shows a total of 8 distinct regions with nonzero probability participating in the inwardly driven conduction process (Figure 4). Conduction proceeds preferentially along the MEP determined from the (0 mV) axial−axial FES, i.e., starting from the state HFS-CEN, ion permeation proceeds sequentially through states CEN[2], CEN-IN, and CEN-CC. Indeed, 85% of the total number of configurations sampled along the trajectories is observed to be in one of these states and forward transition probabilities along the path are at least 1 order of magnitude larger than those relative to alternate routes leading to conduction, e.g., the pathways ending at states HFS-CC or IN-CC (cf. Figure S1).

The axial probability distribution function of the ion k conditioned on the occupancy of each of the states s marking this pathway, $P_k(z|s)$, shows that k is mostly located in the bulk region when the two SF-bound ions are in states HFS-CEN, CEN[2], and CEN-IN (cf. Figure S2). Instead, when the SF-bound ions are in state CEN-CC, a sizable fraction of instantaneous configurations show ion k in regions EX and HFS (21% and 38%, respectively). This demonstrates that the third ion is engaged in permeation only after one of the preceding ones has left the SF.

Overall, the results derived from our voltage-biased simulations through the open channel indicate that, at negative potentials, inward conduction of Na^+ through the selectivity filter of NavAb involves preferentially a two-ion mechanism. The results from the (ΔV) probability distributions support the notion that the latter resembles the process inferred from the FES (based on the closed channel structure at 0 mV).

Outward Conduction and the Role of a Third Ion. In addition to the inwardly driven MD runs, we investigated further the outward transport of ions through NavAb in a series of 8 simulations of the channel under depolarized ($\Delta V > 0$) potentials (cf. methods). Although retaining similar features of the simulations at negative potentials, the depolarized runs show in contrast, an SF-occupancy of ~2.3 ions implying the participation of a third ion in outward conduction (Figures 3 and 4). Starting from the state HFS-CEN, permeation of a pair of ions across the filter follows the same pathway inferred from the (0 mV) FES, i.e., conduction proceeds essentially through HFS[2] and HFS-EX. Note that also in this case the vast majority (98%) of instantaneous configurations are found to populate these states. Computation of $P_k(z|s)$ along this pathway indicates that ion k has a probability of 24% to be located in the filter when the two SF-bound ions are in the state HFS-CEN. $P_k(z|s)$ becomes significantly larger (87%) when the former ions adopt states HFS[2] and EX-HFS. However, in contrast to inward conduction, the strong correlations between the position of k and the SF-bound ions suggests that the

dx.doi.org/10.1021/jp401403b | J. Phys. Chem. B 2013, 117, 3782−3789

outwardly driven transport of ions through the open channel involves a distinct three-ion mechanism, in which a "nudging" collision with an additional cation is required to trigger outward conduction. From the available data, the reasons for this apparent directional asymmetry of the process through the open channel are unclear and further studies will be required to shed light on this topic.

CONCLUSIONS

Two methodologies, metadynamics and voltage-driven MD simulations, have been harnessed to sample rare Na^+ ion channel-crossing events and thereby unravel the conduction mechanism in the NavAb channel. The combination of binding two ions into three stable binding sites of the SF (HFS, CEN, and IN) has revealed five stable configurations. The conduction mechanism involves jumps between these states and whereas a plethora of productive pathways are in principle accessible, we show that most of the permeation events proceed through a minimum FE pathway involving five FE barrier jumps between HFS^2, HFS-CEN, CEN^2, and CEN-IN. This two-ion mechanism can explain the inward conduction of ions through the open channel at negative potentials, but in contrast, under positive potentials, outward conduction seems to involve a distinct three-ion mechanism.

The overall outcome of our work amplifies earlier results that indicate Na^+ conduction operates under a distinct mechanism from K^+ selective channels.[4,6] The latter involves a single file of ion and water molecules, which moves coherently when nudged by a third ion external to the SF thus defining a process involving a bistable (up−down) throughput cycle of two SF-bound K^+ ions.

An important caveat is in order concerning the scope of the present work. First, the calculations were restricted to the conformation of the SF observed in the X-ray structure (the filter structure remains stable in our simulations).[7] Recent studies of K^+ channels have weighed in on the role of conformational flexibility in determining conduction and selectivity.[19,20] In analogy with K^+ channels, both MD trajectories[10] and recent crystal structures of bacterial Na^+ channels[21] suggest that the SF of NavAb shows a significant degree of structural heterogeneity, raising the hypothesis that alternate configurations of the SF may however play a role in conduction and selectivity. Furthermore, given the position of Glu177 at the external entrance of the NavAb-SF structure and thereby its solvent accessibility, the simulation setups relied on the expectation that the pK_a of the side-chain of Glu177 is close to the reference value for the amino-acid in solution and that Glu177 is negatively charged at neutral pH. However, several protonation states are possible for the four titratable side-chains, which may affect conduction and selectivity in NavAb. Indeed, as presented by Corry and Thomas,[11] there seems to be an influence of glutamate protonation on the ion occupancy states of NavAb, suggesting that additional studies are required to address this topic. Finally, it is interesting to set the body of results within the broader context of conduction in Na^+ selective channels. Translating the results of these simulations to eukaryotic channels is not straightforward because the sequence motif of their SF is different. In contrast to K^+ channels, ion conduction in Na^+ channels involves the SF backbone carbonyls as well as their side-chains, making the primary structure of key importance.

Elucidating the molecular determinants of conduction and selectivity is a long-standing goal and involves some of the most fundamental questions in the field of biophysics. Different models have been proposed to rationalize these mechanisms, which emphasize either the different affinity for different species,[22] and/or the ability of sustaining multi-ion concerted displacements.[3] The common trait is, however, the assumption that a well-defined sequence of events underlies conduction. Therefore, the detailed characterization of the ion conduction mechanism within the first structurally characterized sodium selective ion channel holds promise to shed light on the fascinating general problem of conduction and selectivity in biological ion channels, and to ultimately contribute with the key long-term goal of understanding the more complex and pharmacologically relevant mammalian Nav and Cav channels.

METHODS

Molecular Dynamics. The MD simulations were carried out using the program NAMD2.[23] Langevin dynamics was applied to keep the temperature (300 K) fixed. The equations of motion were integrated using a multiple time-step algorithm.[24] Short- and long-range forces were calculated every 1 and 2 time-steps, respectively, with a time step of 2.0 fs. Chemical bonds between hydrogen and heavy atoms were constrained to their equilibrium value. Long-range electrostatic forces were taken into account using the particle mesh Ewald (PME) approach.[25] The water molecules were described using the TIP3P model.[26] The simulation used the CHARMM22-CMAP force field with torsional cross-terms for the protein[27,28] and CHARMM27 for the phospholipids.[29] A united-atom representation was adopted for the acyl chains of the POPC lipid molecules.[30]

Equilibrium Simulation of NavAb. In this contribution, we discuss our previous MD simulations of the reported X-ray crystal structure of NavAb[7] as well as the proposed "fully activated" open conformation of the channel.[15] Details for the NavAb modeling and construction of the macromolecular system can be found in the original papers.[10,15] Briefly, the open structure of NavAb, embedded in a fully hydrated lipid bilayer, was relaxed for ∼35 ns bathed in ∼100 mM NaCl, at constant temperature (300 K) and pressure (1 atm), neutral pH, and with no applied transmembrane (TM) electrostatic potential. An equilibrium ensemble of membrane-equilibrated structures of NavAb, generated by sampling every 0.25 ns from the last 5 ns of the MD trajectory, served as input to a series of independent simulations exploring the conduction of Na^+ through the channel.

Free-Energy Calculations. Since the motion of the ions is restricted to the SF, we use the X-ray structure of NavAb[7] as an initial configuration. The 4-D FE profiles for the two ion permeation events were calculated by metadynamics,[16] using the collective variables module implemented in NAMD.[17] For each ion, two reaction coordinates were chosen: the distance along the pore axis (z-axis) and the radial distance in the plane normal to this axis, i.e., the (x, y) plane, taking in both cases the geometrical center, Cα of the Glu177 residues as a reference. The Gaussian height parameter used to bias the metadynamics runs was 0.3 kcal/mol and the width 0.5 along the z-axis and a 0.25 along the radial dimension, respectively. The space of explored by the z reaction coordinate was restricted to lie within the range −10 to +8 Å by 100 kcal/mol walls. Also, the radial reaction coordinates were limited to a 4 Å radius by the same means. Altogether, the duration of the calculation amounted to 180 ns.

dx.doi.org/10.1021/jp401403b | J. Phys. Chem. B 2013, 117, 3782−3789

To project the 4-D FES onto a 2-D space, we first computed the 4-D probability distribution function at 300 K. From this, we computed the marginal 2-D probability distribution function by integrating over the remaining reaction coordinates and computed therefrom the corresponding FE surface. To recover the minimum FE path linking two FE minima on the axial−axial G(z, z′) surface, we identified the saddle point by using a "modified nudged elastic band" method. Specifically, starting from an initial guess of the string, constituted by a discrete set of points i on the FE surface, we minimized using a Monte Carlo algorithm the following energy function:

$$E = \sum_{i=1}^{N-1} k(l_{i,j+1} - l_0) + G(z_i, z'_i)$$

Here N is the number of points used to describe pathway, k and l_0 are two empirical parameters, $l_{i,j}$ is the distance between two consecutive points along the path, and $G(z_i, z_i')$ is the FE at the ith point as a function of the two axial coordinates. Note that this procedure will favor compact string conformations. The value of N was chosen in order to sample appropriately the roughness of the FES.

Simulations of NavAb under Polarized-Membrane Conditions. To investigate the conduction properties of NavAb under applied voltages, a "fully activated-open" NavAb channel[15] was simulated under polarized-membrane conditions using a charge-imbalance protocol.[18] In this scheme, the channel-membrane system is bathed with ∼100 mM NaCl, and air−water interfaces are then created for electrolytes on each side of the membrane by extending the length of the simulation box in the direction perpendicular to the membrane. Following a short equilibration MD run at constant volume, the system is then simulated under a TM potential imposed by a net-charge imbalance between the upper and lower electrolytes. Since the membrane/channel system behaves as a condenser, the imbalance between the electrolytes creates a potential, ΔV. Here, ΔV is generated by displacing an appropriate number of Na^+ ions from the lower to the upper electrolyte (or vice versa), while keeping the overall concentration of the bulk phases constant.

■ ASSOCIATED CONTENT

Ⓢ Supporting Information

Supplementary Figures. This material is available free of charge via the Internet at http://pubs.acs.org.

■ AUTHOR INFORMATION

Corresponding Author

*(W.T.) Phone: +55.61.3307.2053. E-mail: treptow@unb.br. (V.C.) Phone: +1-215-204-4214. E-mail: vincenzo.carnevale@temple.edu.

Author Contributions

§These authors contributed equally.

Funding

This work was supported in part by the National Institutes for Health and the Commonwealth of Pennsylvania. W.T. thanks the National Council of Technological and Scientific Development (CNPq) for research support (Grant No. 470406/2011-9) and graduate fellowship to L.S. The computations were performed using HPC resources from XSEDE.

Notes

The authors declare no competing financial interest.

■ REFERENCES

(1) Hille, B. *Ionic channels of excitable membranes*, 2nd ed.; Sinauer: Sunderland, MA, 1992.

(2) Shrivastava, I. H.; Tieleman, D. P.; Biggin, P. C.; Sansom, M. S. K^+ versus Na^+ ions in a K channel selectivity filter: a simulation study. *Biophys. J.* **2002**, *83*, 633−645.

(3) Nimigean, C. M.; Allen, T. W. Origins of ion selectivity in potassium channels from the perspective of channel block. *J. Gen. Physiol.* **2011**, *137*, 405−413.

(4) Roux, B. Ion conduction and selectivity in K+ channels. *Annu. Rev. Biophys. Biomol. Struct.* **2005**, *34*, 153−171.

(5) Alam, A.; Jiang, Y. Structural studies of ion selectivity in tetrameric cation channels. *J. Gen. Physiol.* **2011**, *137*, 397−403.

(6) Treptow, W.; Klein, M. L. Computer Simulations of Voltage-Gated Cation Channels. *J. Phys. Chem. Lett.* **2012**, *3*, 1017−1023.

(7) Payandeh, J.; Scheuer, T.; Zheng, N.; Catterall, W. A. The crystal structure of a voltage-gated sodium channel. *Nature* **2011**, *475*, 353−358.

(8) Charalambous, K.; Wallace, B. A. NaChBac: the long lost sodium channel ancestor. *Biochemistry* **2011**, *50*, 6742−6752.

(9) Burykin, A.; Kato, M.; Warshel, A. Exploring the origin of the ion selectivity of the KcsA potassium channel. *Proteins* **2003**, *53*, 412−426.

(10) Carnevale, V.; Treptow, W.; Klein, M. L. Sodium Ion Binding Sites and Hydration in the Lumen of a Bacterial Ion Channel from Molecular Dynamics Simulations. *J. Phys. Chem. Lett.* **2011**, *2*, 2504−2508.

(11) Corry, B.; Thomas, M. Mechanism of Ion Permeation and Selectivity in a Voltage Gated Sodium Channel. *J. Am. Chem. Soc.* **2012**, *134*, 1840−1846.

(12) Furini, S.; Domene, C. On Conduction in a Bacterial Sodium Channel. *PLoS Comput. Biol.* **2012**, *8*, e1002476.

(13) Qiu, H.; Shen, R.; Guo, W. Ion solvation and structural stability in a sodium channel investigated by molecular dynamics calculations. *Biochim. Biophys. Acta* **2012**, *1818*, 2529−2535.

(14) Zhang, X.; Xia, M.; Li, Y.; Liu, H.; Jiang, X.; Ren, W.; Wu, J.; Decaen, P.; Yu, F.; Huang, S.; He, J.; Clapham, D. E.; Yan, N.; Gong, H. Analysis of the selectivity filter of the voltage-gated sodium channel Na(v)Rh. *Cell Res.* **2012**, *23*, 409−422.

(15) Amaral, C.; Carnevale, V.; Klein, M. L.; Treptow, W. Exploring conformational states of the bacterial voltage-gated sodium channel NavAb via molecular dynamics simulations. *Proc. Natl. Acad. Sci. U.S.A.* **2012**, *109*, 21336−21341.

(16) Laio, A.; Gervasio, F. L. Metadynamics: a method to simulate rare events and reconstruct the free energy in biophysics, chemistry and material science. *Rep. Prog. Phys.* **2008**, *71*, 126601.

(17) Hénin, J.; Fiorin, G.; Chipot, C.; Klein, M. L. Exploring Multidimensional Free Energy Landscapes Using Time-Dependent Biases on Collective Variables. *J. Chem. Theory Comput.* **2010**, *6*, 35−47.

(18) Delemotte, L.; Dehez, F.; Treptow, W.; Tarek, M. Modeling membranes under a transmembrane potential. *J. Chem. Phys. B* **2008**, *112*, 5547−5550.

(19) Noskov, S. Y.; Bernèche, S.; Roux, B. Control of ion selectivity in potassium channels by electrostatic and dynamic properties of carbonyl ligands. *Nature* **2004**, *431*, 830−834.

(20) Bostick, D. L.; Brooks, C. L., 3rd Selectivity in K+ channels is due to topological control of the permeant ion's coordinated state. *Proc. Natl. Acad. Sci. U.S.A.* **2007**, *104*, 9260−9265.

(21) McCusker, E. C.; Bagnéris, C.; Naylor, C. E.; Cole, A. R.; D'Avanzo, N.; Nichols, C. G.; Wallace, B. A. Structure of a bacterial voltage-gated sodium channel pore reveals mechanisms of opening and closing. *Nat. Commun.* **2012**, *3*, 1102.

(22) Bernèche, S.; Roux, B. Energetics of ion conduction through the K+channel. *Nature* **2001**, *414*, 73−77.

(23) Phillips, J. C.; Braun, R.; Wang, W.; Gumbart, J.; Tajkhorshid, E.; Villa, E.; Chipot, C.; Skeel, R. D.; Kale, L.; Schulten, K. Scalable molecular dynamics with NAMD. *J. Comput. Chem.* **2005**, *26*, 1781−1802.

(24) Izaguirre, J. A.; Reich, S.; D, S. R. Longer time steps for molecular dynamics. *J. Chem. Phys.* **1999**, *110*, 9853−9864.
(25) Darden, T.; York, D.; Pedersen, L. Particle mesh Ewald - An Nlog(N) method for Ewald sums in large systems. *J. Chem. Phys.* **1993**, *98*, 10089−10092.
(26) Jorgensen, W. L.; Chandrasekhar, J.; Madura, J. D.; Impey, R. W.; Klein, M. L. Comparison of simple potential functions for simulating liquid water. *J. Chem. Phys.* **1983**, *79*, 926−935.
(27) MacKerell, A. D., Jr.; Bashford, D.; Bellott, M.; Dunbrack, R. L., Jr.; Evanseck, J.; Field, M. J.; Fischer, S.; Gao, J.; Guo, H.; Ha, S.; Joseph-McCarthy, D.; Kuchnir, L.; Kuczera, K.; Lau, F. T. K.; Mattos, C.; Michnick, S.; Ngo, T.; Nguyen, D. T.; Prodhom, B.; Reiher, W. E., III; Roux, B.; Schlenkrich, M.; Smith, J. C.; Stote, R.; Straub, J.; Watanabe, M.; Wiorkiewicz-Kuczera, J.; Yin, D.; Karplus, M. All-atom empirical potential for molecular modeling and dynamics studies of proteins. *J. Phys. Chem. B* **1998**, *102*, 3586−3616.
(28) MacKerell, A. D., Jr.; Feig, M.; Brooks, C. L., III Improved Treatment of the Protein Backbone in Empirical Force Fields. *J. Am. Chem. Soc.* **2004**, *126*, 698−699.
(29) Feller, S. E.; MacKerell, A. D., Jr. An improved empirical potential energy function for molecular simulations of phospholipids. *J. Phys. Chem. B* **2000**, *104*, 7510−7515.
(30) Hénin, J.; Shinoda, W.; Klein, M. L. United-atom acyl chains for CHARMM phospholipids. *J. Chem. Phys. B* **2008**, *112*, 7008−7015.